

AN INITIAL ASSESSMENT OF THE EFFECTS OF INCREASED NI AND V CONTENT IN A356 AND AA6063 ALLOYS

¹John Grandfield, ²Lisa Sweet, ²Cameron Davidson, ²Jason Mitchell, ²Aiden Beer, ²Suming Zhu, ²Xiaobo Chen, ²Mark Easton:
¹ Grandfield Technology, Brunswick, Victoria 3055, Australia and ² CAST, Clayton, Victoria, Australia

Keywords: Nickel, vanadium, petroleum coke, A356, A601, Al-7Si-Mg, AA6063, AA6060, alloy properties

Abstract

Changes in calcined coke composition associated with different crude oil sources have caused nickel (Ni) and vanadium (V) levels in aluminum to rise. To ensure cast product quality is not compromised an understanding of the effects of these changes is needed. An initial investigation has been conducted for two commonly used alloys, A356 and AA6060/6063. Castings were produced with low typical levels of Ni-V and with high Ni-V levels approaching the maximum P1020 specification of 300ppm each. Microstructural changes were assessed using optical and scanning electron microscopy and tensile properties and corrosion resistance were measured. For as-cast A356 alloy, there was no significant difference in corrosion performance, but adding Ni and V had a small effect on tensile properties. For AA6060/6063 alloy there was no significant difference in the tensile properties of extrusions with low and high Ni-V levels but a small drop in corrosion performance was measured at high Ni-V levels.

Introduction

Aluminum smelters and anode coke suppliers are formulating strategies to tackle increasing metal impurity (nickel, Ni and vanadium, V) concentrations arising from changes in petroleum coke (PET coke) quality. As smelter demand outstrips the supply of low V/Ni green coke sources, the average levels of these metal impurities in anodes and in smelter metal is creeping up [1-4].

As sweet crude becomes scarcer and more sour crude is used in petroleum coke production, levels of Ni and V in coke have risen ~10-20 ppm per annum in the last decade. Of late, switches in crude supplier are causing large jumps of 100 ppm. Green cokes of 600 ppm V are routinely being blended into the calcined coke supply now and levels may go as high as 1000-2000 ppm at some stage in the future. The amount of Ni and V that partitions to the aluminum varies according to cell operations but typically half goes to the metal.

Current specifications for Ni and V seem to have been set according to the smelter melt compositions that have historically been achieved rather than exact knowledge of the effect of the elements at dilute levels; the exception being electrical conductivity grade alloys where there are clearly documented detrimental effects of V. To establish if specifications can be widened, test work is required to measure key properties e.g. corrosion, strength, fatigue, extrudability, surface finish, anodising response.

RAIN CII and BHP Billiton commissioned CAST CRC to conduct a project examining options for impurity control along the value chain from PET coke to final alloy products. This work included a literature review and preliminary metallurgical and property measurements on two common alloys to show the effect of Ni and V concentration.

Alloy Specifications

The LME (London Metals Exchange) specification for typical P1020A high grade 99.7% aluminum are <0.10% Si, <0.20% Fe, and <0.03% V while Ni falls under the 0.03% maximum for each of the other elements. Note that the total others is 0.1%. Note also that when expressed in ppm, the levels are adjusted for rounding thus 0.03% becomes 349 ppm not 300ppm.

The LME casting alloy specifications are generally wider; e.g. A380 alloy has Ni 0.5% max, total others 0.5%. Aluminum Association unalloyed grades can be tighter e.g. for P0202A with <0.01% V, <0.02% Ga, Si, Fe and Zn and <0.01 % others each.

Smelters and customers negotiate specifications for specific products that are tighter than the LME specifications and these vary around the world. Japanese customers for example tend to have tight Ni specifications e.g. <80ppm Ni on ingot for wheel alloys because of corrosion concerns.

Some smelter products such as some electrical conductivity grade alloys have very tight specifications of down to <10 ppm for V, Cr, Ti and Mn but in general where there is a specification it is between 100 ppm and 300 ppm.

For some alloys, e.g. the 6xxx series, most plants do not have a specification for maximum Ni or V levels. Nickel is often not itemized in reported analyses and is lumped under others. Vanadium is more often specified than Ni.

In the short term, some smelters are now having difficulty meeting the 100 ppm V specification on some alloys.

In the long term, with the prospect of V concentration in coke rising to 1000 ppm and corresponding metal levels increasing to around 500 ppm, the LME P1020 specifications could also be exceeded if no steps are taken to remove Ni and V.

Published information on the Effects of Ni and V

Because Ni and V are not normally used as alloying elements due to their high cost, their metallurgy and their effect on properties has not been examined as extensively as the common alloying elements.

Grandfield & Taylor [5, 6] recently reviewed the literature on Ni and V effects on properties. Little work has been published on the effects in the 100-1000 ppm range. Most known Ni effects are at the order of 1% addition and include;

- Electrical conductivity [7]
- Stiffness [8]
- Strength [7]
- Wear resistance [9]

Here we present a selection from the literature review relating to the effects of Ni and V where these elements are considered impurities rather than deliberate additions.

Effects of Ni

Generally, in aluminum alloy systems with low Ni levels, the Ni will mainly be associated with iron, i.e. in AlFeSi intermetallics. Nickel is a slow diffusing element and therefore the matrix is likely to contain levels below the equilibrium solubility due to microsegregation i.e. most of the Ni will go to the intermetallics at the grain boundaries. The corrosion resistance is somewhat reduced by Ni additions, but in aluminum 99.99% or better, especially if exposed to high-temperature water or steam, Ni alone or together with iron has a beneficial effect on corrosion resistance [8]. In dilute alloys such as 1100, Ni promotes pitting corrosion [7]. Aluminum destined for alloying into magnesium requires low Ni because Ni causes corrosion in Mg alloys at levels above 5ppm [10]. Nickel can also have some effect on “fir tree” grain structure in 1xxx series alloys and give unwanted variation in anodizing response. It has also been shown to have a negative effect in die soldering during pressure die casting [11].

Effects of V

Vanadium is a peritectic element with a very low diffusion coefficient. The maximum solid solubility of V in aluminum is ~0.4wt% and occurs at the peritectic temperature [11], although V containing intermetallic particles are unlikely to form at concentrations below 1000 ppm [12]. Vanadium is reported to have a small beneficial grain refining effect [8] although it is less efficient than Ti or Zr [7]. In the presence of the conventional titanium boride-based grain refiners it seems to have no effect in EC grade aluminum [13] or 99.5% Al [14].

Corrosion resistance is little affected by V and the slight increase is consistent with grain refinement [8].

V may form dispersoids in Al-Mg-Si alloy, but for additions of up to 0.1 wt. % and possibly higher no appreciable amount of dispersoids is formed [15]. However, the combination of 0.1% V or 0.1% Mn together leads to a marked increase in the number of dispersoids after homogenisation. The influence of V alone is relatively small compared with that of Mn alone or the combination of Mn and V [14]. It is suggested that V may promote precipitation of α -phase during high temperature treatments in regions where it might otherwise have difficulty in forming. Conditions that influence the formation of the α -phase e.g. purity level, Mn content, Si content, Fe: Si ratio and soaking conditions will influence the extent to which V influences properties [14].

The grain size is reported to be finer in a hot rolled and annealed AlMgSi alloy with a Mn addition, but finest when both V and Mn are present [14]. The addition of both V and Mn promotes the formation of a structure that is more resistant to coarse grain formation during recrystallisation. This has been observed in heavily deformed, thinner gauge rolled material [14] and in medium strength AlMgSi extrusion alloys [16]. It can also prevent the formation of orange peel during cold forming of extrusions or forgings [12].

Vanadium has been reported to affect the color tone of clear anodized sheet if sufficient manganese is also present to boost the influence of V in forming a higher density of α -phase particles

[12]. High levels of V in solution will reduce the deformation resistance or extrudability of the alloy [15].

The main detrimental effect of V is the reduction in electrical conductivity that occurs. The electrical resistivity increases 3.58 $\mu\Omega$ -cm for every 1% V added in solution or 0.28 $\mu\Omega$ -cm out of solution [7]. For example, V in solution at 0.0138% decreases electrical conductivity by 1.0% IACS [17]. The effect of V in solution on conductivity is included below - 100 ppm of V appears to reduce conductivity by the order of 0.7% IACS [13]. For metal that is destined for production of electrical grade alloys this necessitates V removal using boron treatment

Investigation

Two large volume alloys, AA6063 and A356 were tested without Ni and V additions and with Ni and V additions to achieve a target value of 300ppm each. Sample compositions are given in Table 1 & 2. 10%V and 5%Ni master alloys were used for the additions. The 6xxx series alloy composition falls within the AA6060 and AA6063 specifications; the most common 6xxx series alloys and will be referred to as AA6063.

A356 alloy with Ni (24ppm) and V (110ppm) levels similar to typical smelter analysis was prepared and cast into molds to create samples for microstructural analysis, corrosion and tensile testing. Ni and V were added to this alloy to create an A356 Ni-V alloy with 290 ppm Ni and 263 ppm V (Table 2) which was also corrosion and tensile tested.

The A356 samples for characterization were cut from the casting plates and were subjected to a standard T6 heat treatment, i.e. solution treated at 540 °C for 6 hrs, quenched into hot water (~60 °C), and then aged at 160 °C for 4 hrs. After heat treatment the A356 samples were machined into tensile test specimens.

The AA6063 samples were extruded at Deakin University using a laboratory-scale extrusion press and given a T6 heat treatment (solution treated at 575 °C for 2.5 hrs and aged at 190 °C for 6 hrs). Three extrusions were made of each AA6063 alloy and three tensile test samples prepared from each extrusion. Extrusion was carried out at 540°C and 15m/s extrusion speed. Tensile tests were conducted at a strain rate of 0.001/s. Samples were examined using scanning electron microscopy (SEM) and optical microscopy. After mechanical grinding to a 2400 grit SiC finish, the samples were carefully polished using 0.05 μm silica suspension for ~10 minutes and 0.05 μm alumina suspension for ~2 minutes. Without chemical etching, the polished samples were examined in a JEOL JSM 7001F field emission SEM, equipped with an HKL Channel 5 EBSD system and a Bruker Quantax EDX system.

For corrosion testing the AA6063 samples were hot rolled at Deakin University. The 16mm thick as-cast samples were milled to 11mm to remove the casting surface. The material was preheated to 450°C and held for 30 minutes. An initial roll pass reduced the thickness to 5.2mm before returning to the furnace for 10 minutes at 450°C and a second roll pass further reduced the thickness down to 2.4mm. After rolling the samples were allowed to air cool. The A356 samples were prepared from the as cast T6 samples. Linear Polarization Resistance and salt spray tests were carried out on the samples.

Table 1 Compositions of the AA6063 alloy samples as determined by ICP analysis.

| Sample | Ni (ppm) | V (ppm) | Si (%) | Mg(%) | Fe(%) | Mn(%) | Ti(%) |
|-----------------|----------|---------|--------|-------|-------|-------|-------|
| AA6063 Standard | 60 | 140 | 0.40 | 0.45 | 0.17 | 0.04 | 0.015 |
| AA6063 Ni-V | 300 | 260 | 0.42 | 0.46 | 0.19 | 0.04 | 0.014 |

Table 2 Compositions of the A356 alloy samples as determined by optical emission spectroscopy (OES).

| Sample | Ni (ppm) | V (ppm) | Si | Mg | Fe | Ti |
|---------------|----------|---------|------|-------|-------|-------|
| A356 standard | 24 | 100 | 7.5 | 0.372 | 0.135 | 0.096 |
| A356 Ni-V | 290 | 300 | 7.63 | 0.374 | 0.138 | 0.095 |

Results

A356 Microstructures

There was no detectable difference in the as cast secondary dendrite arm spacing between the A356 base alloy and the alloy with the higher Ni and V levels. A356 typically forms with initial solidification of Al-rich dendrites to approximately 50 vol% solid, followed by a binary Al-Si eutectic, and then by higher order eutectic containing Al, Si with some combination of Mg₂Si, AlFeSi phases and π -AlSiFeMg, depending on composition and cooling rate. The binary Si morphology did not show any dependence on Ni or V levels.

The optical micrograph in Figure 1 shows a sample microstructure from the slower cooled region of the wedge casting, with the major phases indicated, as identified by scanning electron microscopy/ X-ray analysis. The script phases could have been π or α -AlFeSi, but the presence of Mg in almost all of the particles examined in the SEM showed they were π -phase. Mg₂Si was present at only a very small fraction, and only a single particle of AlFeSi was observed in the slower cooled region.

Near the casting tip, or the wall, where overall freezing rates were significantly higher, the relative fraction of minor phases was rather different. The differences were apparent under the optical microscope (Figure 2), and confirmed in the SEM. There was significantly more Mg₂Si and AlFeSi present. From the plate-like morphology it is likely that the AlFeSi was the β -phase. The alloy with high Ni and V showed the same trends as the base alloy in terms of there being more β -AlFeSi and Mg₂Si in the faster cooled regions, and more π -phase in the slower-cooled region. All the significant phases is shown in Figure 3.

The Ni was found to be mainly present in the π -phase, plus there was a small number of very small particles with very high Ni, moderate Si, minor amounts of Mg (~1 wt%) and no detectable Fe. This has been labelled in Figure 3 as AlSiNi, but the stoichiometry is not known and the Ni:Si ratio shows a wide variability, suggesting that there was scatter from X-rays from particles external to this phase. The particles were only 2-5 μ m across and therefore very difficult to analyse accurately. SEM micrographs of the heat-treated microstructures are shown in Figure 4 and is typical of what has been published elsewhere (Mark reference?) for alloys with low to moderate levels of Mg: After heat-treatment the Mg goes into solution, causing any Mg₂Si to dissolve and the majority of the π -phase is converted to very small β -plates and a globular phase.

SEM with electron backscatter diffraction (EBSD) found that in the heat treated condition three phases were present in both the standard alloy and Ni-V alloy, namely π -phase, β -phase and α -phase. Ni was detected in all three phases. However, it has been determined that the majority of the Ni in the Ni-V alloy is found in α -Al₁₉Fe₄MnSi₂ phase. Typical SEM secondary electron image (SEI), EBSD pattern, and EDX analyses of this intermetallic phase are shown in Figure 5 and Figure 6 for the standard A356 alloy and A356 Ni-V alloy respectively.

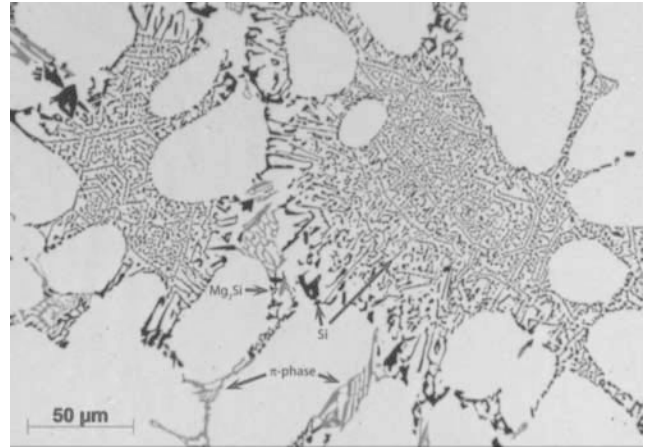


Figure 1 Typical optical microstructure in slow-cooled region of base Al-7Si-Mg alloy.

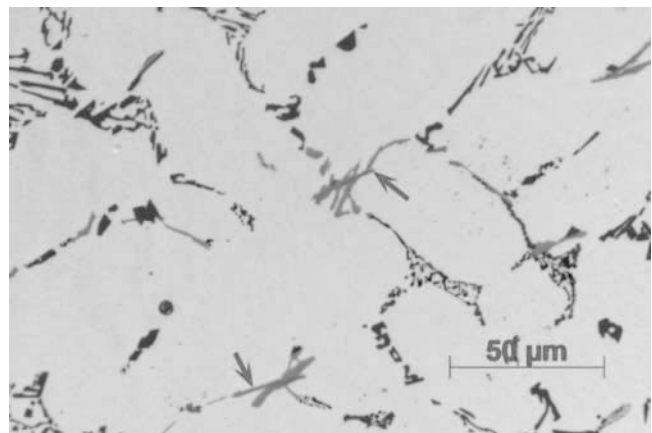


Figure 2 Microstructure of base alloy closer to chill surface, showing central AlFeSi phase (probably β) with π -phase (slightly blueish) phase apparently growing from it.

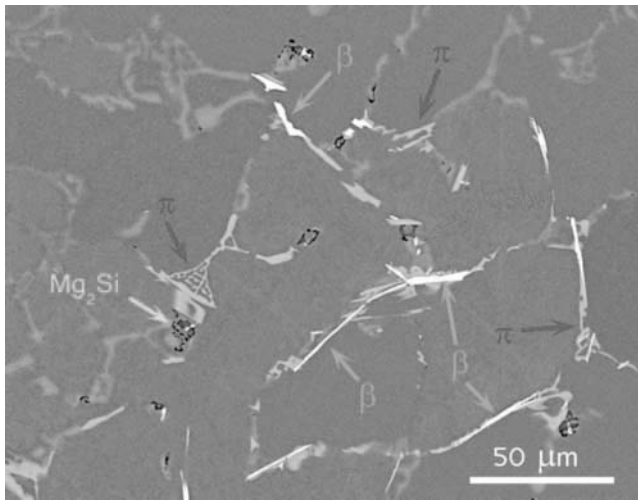


Figure 3 Backscattered SEM image showing typical forms of all minor phases. Image taken near chill surface.

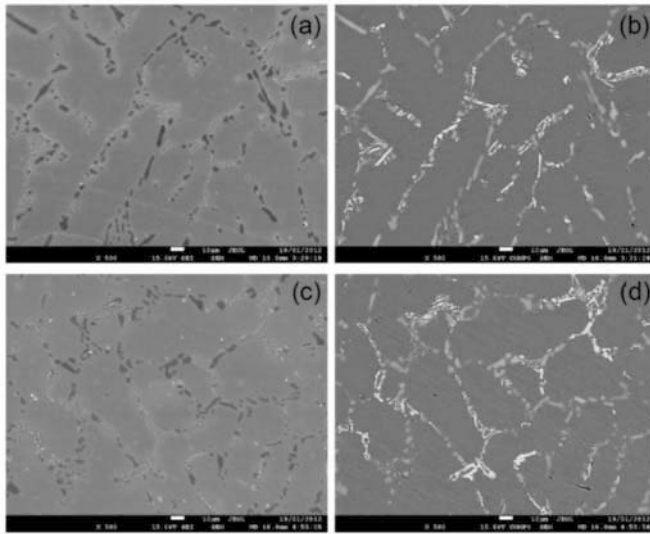


Figure 4 SEM (a and c) and BSE images (b and d) showing general microstructure of heat treated A356 alloys (a and b) A356 standard and (c and d) A356 Ni-V. Particles in grey in (b) and (d) are primary Si phase whilst those with high contrast are intermetallic phases.

The presence of extra V in the A356 alloy had no observable effect on the microstructure, in either in the as-cast or heat-treated states.

AA6063 Microstructures

For the extruded AA6063 alloy, the intermetallic phases were identified to be either hexagonal α -AlFeSi or body-centred cubic α -AlFeSi in both the standard and Ni-V alloy. Using SEM with electron backscatter diffraction (EBSD) Ni was detected in both phases. However, it has been determined that the majority of the Ni in the Ni-V alloy is found in α -Al₁₉Fe₄MnSi₂ phase. Typical SEM secondary electron image (SEI), EBSD pattern, and EDX analyses of this intermetallic phase are shown in Figure 7 and Figure 8 for the standard A356 alloy and A356 Ni-V alloy respectively.

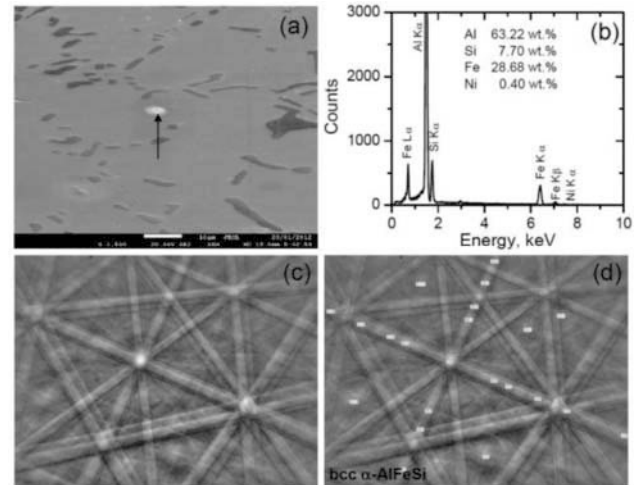


Figure 5 Identification of intermetallic phase (arrowed) in the heat treated A356 standard alloy by EBSD: (a) SEM secondary electron image, (b) EDX spectrum, (c) raw EBSD pattern, and (d) EBSD pattern indexed according to α -Al₁₉Fe₄MnSi₂ (body centred cubic, $a = 1.256$ nm).

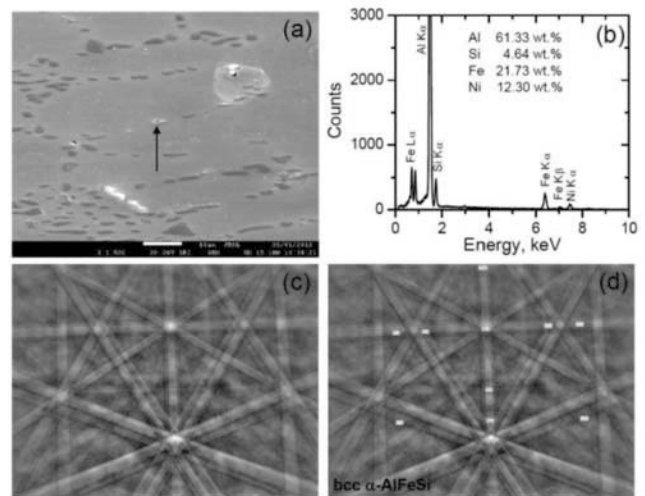


Figure 6 Identification of intermetallic phase (arrowed) in the heat treated A356 Ni-V alloy by EBSD: (a) SEM, (b) EDX spectrum, (c) raw EBSD pattern, and (d) EBSD pattern indexed according to α -Al₁₉Fe₄MnSi₂ (body centred cubic, $a = 1.256$ nm). The Ni level in α -Al₁₉Fe₄MnSi₂ is significantly higher in this alloy compared to the standard alloy.

The presence of extra V in the AA6063 alloy had no observable effect on the extruded microstructure.

Mechanical Properties

Preliminary data (2 tests per alloy) indicated that there was a slight drop in strength for the A356 alloy with high Ni-V and possibly no change in the ductility (Figure 9). Further testing is required to confirm this result.

No statistically significant difference in tensile strength or elongation was observed between the standard and high Ni-V AA6063 alloys (Figure 10). Student t tests indicate low probability of the two alloys having a different mean values.

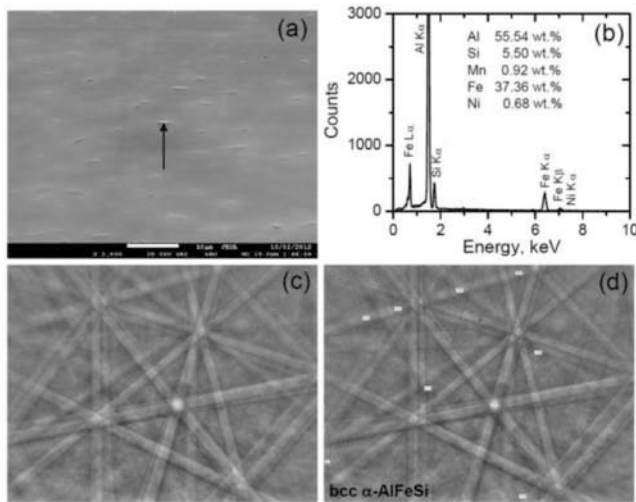


Figure 7 Identification of intermetallic phase (arrowed) in extruded AA6063 standard alloy by EBSD: (a) SEM secondary electron image, (b) EDX spectrum, (c) raw EBSD pattern, and (d) EBSD pattern indexed according to α -Al₁₉Fe₄MnSi₂ (body centred cubic, a = 1.256 nm).

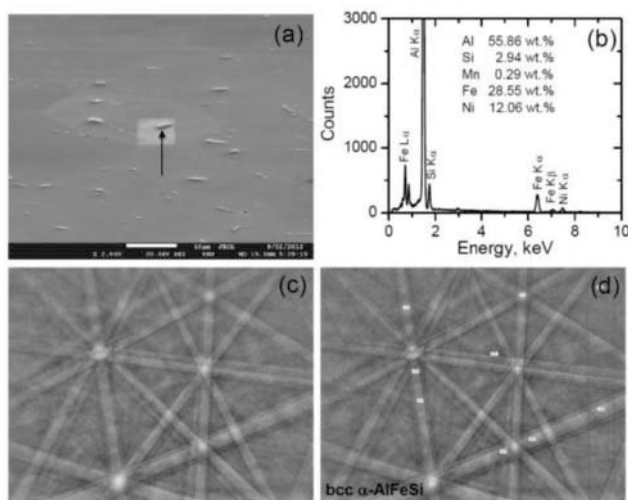


Figure 8 Identification of intermetallic phase (arrowed) in extruded AA6063 Ni-V alloy by EBSD: (a) SEM, (b) EDX spectrum, (c) raw EBSD pattern, and (d) EBSD pattern indexed according to α -Al₁₉Fe₄MnSi₂ (body centred cubic, a = 1.256 nm). The Ni level in α -Al₁₉Fe₄MnSi₂ is significantly higher in this alloy compared to the standard alloy.

No difference was measured in peak load during extrusion between the standard and high Ni-V AA6063 alloys.

Corrosion

Normally, polarisation curves depict the corrosion progress of the tested alloys in corrosive medium, such as 0.1 M NaCl. The corrosion potential (E_{corr}) and corrosion current density (i_{corr}) are calculated via the Tafel slope fitting technique. It can be seen that the E_{corr} decreases about 10 mV and 110 mV for A356 and AA6063 with the Ni-V addition, respectively.

There is no significant difference in the corrosion current between the two A356 alloys, i_{corr} of A356 (8.36×10^{-4} Amp/cm²) and A356

Ni-V (9.18×10^{-4} Amp/cm²). However, with the addition Ni and V to the AA6063 alloy, there is a measured increase in corrosion current from 1.2×10^{-6} Amp/cm² (AA6063) to 1.5×10^{-5} Amp/cm² (AA6063 Ni-V) by adding into this alloy (Figure 11). This result suggests that the addition of Ni and V has very little effect on the corrosion resistance of A356 and a minor, but significant deleterious effect on the AA6063 alloy.

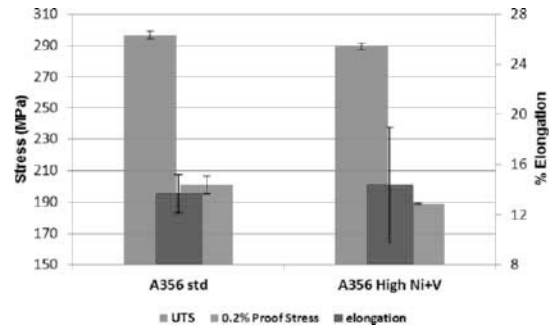


Figure 9 Bar chart of mean (average of two tests) T6 A356 tensile properties and standard deviation showing the effect of Ni-V impurity content.

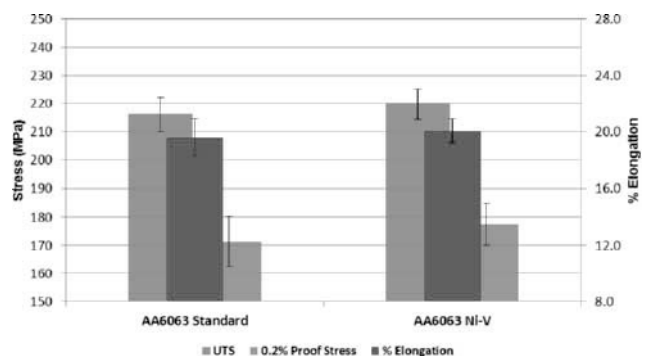


Figure 10 Bar chart of mean (average of five tests) T6 AA6063 tensile properties and standard deviation showing the effect of Ni-V impurity content.

The difference in the corroded area of the surfaces of A356 and A356 Ni-V, AA6063 and AA6063 Ni-V is not significant when comparing the photograph taken after salt spray test from 1 hour to 48/96 hours (Error! Reference source not found. and Error! Reference source not found.). Hence although the polarisation results indicated that there may be a small difference in the corrosion response of the AA6063 alloys in particular, the salt spray test was not able to differentiate between them.

Summary

For both the AA6063 and 356 alloys, Ni tends to partition into the intermetallic phases, especially the body-centred cubic α -AlFeSi. Higher levels of Ni were measured in the intermetallic phases for the Ni-V added alloys compared to the standard alloys. For both alloys, V probably resides in the Al matrix as solute. No increased V levels were detected in the intermetallic phases for the Ni-V added alloys. The results indicate no effect of Ni and V on mechanical properties at the high concentration level tested on the AA6063 alloy tested however there is a small but deleterious effect on corrosion performance.

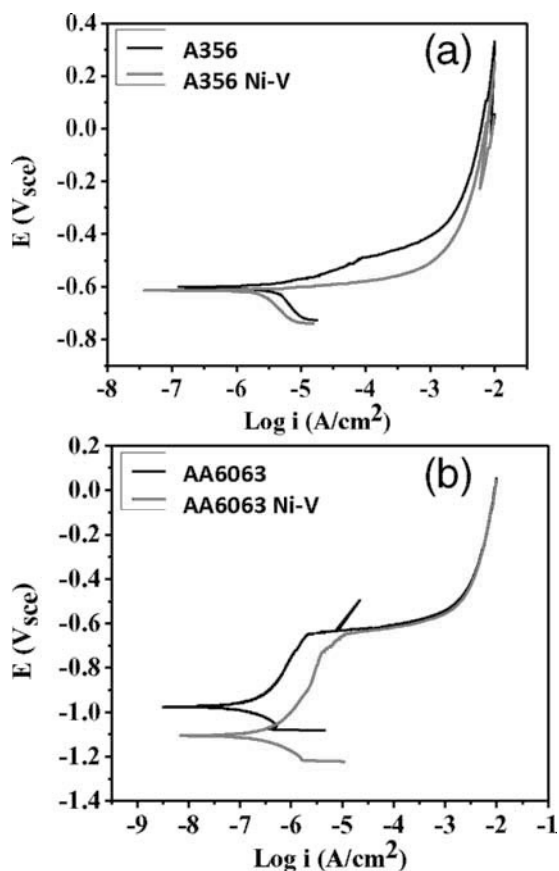


Figure 11 Polarisation curves of (a) A356 and A356 Ni-V alloys and (b) AA6063 and AA6063 Ni-V alloys.

While the corrosion performance of the A356 was not different between the base alloy and the high NiV alloy, there may be a reduction in mechanical properties in the A356 alloy due to Ni-V additions.

At this stage with the limited data it is not possible to understand the mechanisms of how Ni and V are affecting the properties. Without further testing at intermediate levels, the critical concentration at which the effects of Ni and V take effect is not known.

Conclusions

Given these results, it would appear there may be scope to allow some increase in Ni and V levels within the P1020 specification however not up to the limits of the specification. Caution is warranted and further testing is needed to determine the exact tolerance limits and to separate out the effects of Ni and V.

References

1. F. Vogt et al., *A Preview of Anode Coke Quality in 2007*, in *TMS Light Metals*, A.T. Tabereaux, Editor. 2004: Charlotte, NC. p. 489-493.

2. L. Edwards, *Responding to Changes in Coke Quality*, in *9th Australian Smelting Conference*. 2008, B. Welch, Skyllas-Kazacos, M.: Terrigal, NSW.
3. L. Edwards, *Evolution of Anode Grade Coke Quality and Calcining Technology*, in *10th Australian Smelting Conference*, G.S. B. Welch, J. Metson, M. Skyllas-Kazacos Editor. 2011, Uni. NSW. p. 2a1.
4. L. Edwards, F. Vogt, and J. Wilson, *Coke Blending at Anglesey Aluminium*, in *Light Metals: Proceedings of Sessions, TMS Annual Meeting (Warrendale, Pennsylvania)*, J. Anjier, Editor. 2001: New Orleans, LA. p. 689-694.
5. J. Grandfield and J. A. Taylor, "The Impact of Rising Ni and V Impurity Levels in Smelter Grade Aluminium and Potential Control Strategies," *Aluminium Cast House Technology, 11th Australasian Conference and Exhibition, September 13, 2009 - September 16, 2009*, (Trans Tech Publications Ltd, 2010), 129-136.
6. J. F. Grandfield et al., *Melt Quality and Management of Raw Material Impurities in Cast House*, in *10th Australian Smelting Conference*, G.S. B. Welch, J. Metson, M. Skyllas-Kazacos Editor. 2011, Uni. NSW: Launceston, Tasmania. p. 1c2.
7. J. E. Hatch, *Aluminum: Properties and Physical Metallurgy*. 1984, Metals Park, Ohio: American Society for Metals.
8. L. F. Mondolfo, *Aluminum Alloys: Structure and Properties*. 1976, Butterworths: Boston.
9. N. A. Belov and V. S. Zolotarevskiy, *The Effect of Nickel on the Structure, Mechanical and Casting Properties of Aluminium Alloy of 7075 Type*, in *Materials Science Forum*, P.J. Gregson and S. Harris, Editors. 2002: Cambridge. p. 935-940.
10. I. J. Polmear, "Magnesium Alloys and Applications," *Materials Science and Technology*, 10 (1)(1994), 1-16.
11. I. J. Polmear, *Light Alloys (Fourth Edition)*, (Oxford: Butterworth-Heinemann, 2005).
12. U. Mannweiler et al., *High Vanadium Venezuelan Petroleum Coke, a Rawmaterial for the Aluminum Industry?*, in *Light Metals: Proceedings of Sessions, AIME Annual Meeting (Warrendale, Pennsylvania)*. 1989, Publ by Metallurgical Soc of AIME: Las Vegas, NV, USA. p. 449-454.
13. R. Cook, M. A. Kearns, and P. S. Cooper, *Effects of Residual Transition Metal Impurities on Electrical Conductivity and Grain Refinement of Ec Grade Aluminum*, in *Light Metals: Proceedings of Sessions, TMS Annual Meeting (Warrendale, Pennsylvania)*. 1997, Minerals, Metals & Materials Soc (TMS): Orlando, FL, USA. p. 809-814.
14. A. H. R. Maitland, D., *Vanadium in Aluminium*, in *8th Internationale Leichtmetalltagung*. 1987. p. 423-425.
15. T. Furu et al., "Aluminium Alloy with Improved Crush Properties" (Patent 20090116999, 2009).
16. P. Z. Schwellinger, H and A. Maitland, *Medium Strength Almgis Alloys for Structural Applications*, in *ET 1984: Third International Aluminum Extrusion Technology Seminar*, A.E. Council, Editor. 1984, ET Foundation: Atlanta, Georgia, U.S.A. p. 17-20.
17. S. Karabay, "Modification of Aa-6201 Alloy for Manufacturing of High Conductivity and Extra High Conductivity Wires with Property of High Tensile Stress after Artificial Aging Heat Treatment for All-Aluminium Alloy Conductors," *Materials & Design*, 27 (10)(2006), 821-832.

Acknowledgement

CAST and Grandfield Technology gratefully acknowledge the financial support of BHPBilliton and RAIN CII and permission to

publish this work. The authors gratefully acknowledge Monash Centre for Electron Microscopy (MCEM) for access to experimental facilities.